

(Amersham Pharmacia). The plasmid was then used to transform *Escherichia coli* BL21, and expression of the fusion protein was induced by adjusting the culture to 1 mM Isopropyl- β -D-thiogalactopyranoside (IPTG). The fusion protein was purified using a glutathione-Sepharose 4B column (Amersham Pharmacia). The kinase reaction products were boiled in sample buffer and analyzed by SDS-PAGE.

Antibodies

Antibodies to Mus81 (N-20), cyclin A (C-19), cyclin E (C-19), cyclin B1 (GNS1), Cdc2 (Cdk1) (17), Cdk2 (D-12), Chk2 (A-12), Chk1 (G-4), ATR (N-19) and actin (C-2) were from Santa Cruz Biotechnology. Antibodies to phospho-Chk2 (Thr-68), phospho-Chk1 (Ser-317) and p21 (DCS60) were from Cell Signaling Technology. The antibody to ATM (NB100-104) was from Novus Biologicals.

Immunofluorescence

Cells were grown overnight on coverslips and fixed for 10 min in 4% paraformaldehyde. Cells were blocked with 10% horse serum and incubated with primary antibodies at room temperature for 1 h and with secondary antibodies for 30 min. Finally, cells were counterstained with 4',6'-diamidino-2-phenylindole (DAPI) and mounted.

siRNA transfection

Eight hours prior to transfection, cells for the assay of ATM and ATR expression were seeded in a 100 mm dish at 1×10^6 cells/dish. Cells for immunofluorescence were seeded on coverslips at 1×10^5 cells/coverslip. The siRNA sequences for ATM used in the study were 5'-CAUCUAGAUCGGC-AUUCAGtt-3' and 5'-UGGUGCUAUUUAAACGGAGCtt-3'. The siRNA sequence for ATR was 5'-AACCUCGUGAU-GUUGCUUGAtt-3'. These siRNAs were synthesized by Sigma Genosys. A siCONTROL nontargeting siRNA from Dharmacon was used as a negative control. Transfection was performed using Lipofectamine 2000 transfection reagent (Invitrogen) according to the manufacturer's instructions. For western blot analysis, the Lipofectamine-siRNA complex was not removed during incubation. Cells were harvested at 48 h post-transfection. For immunofluorescence after double-thymidine block, the transfection mixture was removed after the first thymidine block.

Ectopic expression of Cdk1

The human *Cdk1* cDNA was amplified by PCR from cDNA derived from normal human cells using primers 5'-GCTCTT-GGAAATTGAGCGGA-3' and 5'-AGAAGACGAAGTACA-GCTGAAGT-3'. The cDNAs were inserted into pCR2.1, and the sequences were confirmed. The *Cdk1* expression vector was designed to insert the gene under the control of the MSV enhancer and the MMTV promoter. *Cdk1*-overexpressing cells were selected in the presence of 900 μ g/ml ZeocinTM (Invitrogen).

RESULTS

Generation of Mus81-deficient HCT116 cells

To investigate Mus81 function in human cells, we inactivated its gene in HCT116 cells by gene targeting. Targeting vectors

were designed such that exon 3 was disrupted by promoterless antibiotic-resistance genes (Figure 1A). We obtained two independent *Mus81*^{+/-} clones from 744 neomycin-resistant colonies and two *Mus81*^{-/-} clones from 2380 neomycin- and blasticidin-resistant colonies derived from a single *Mus81*^{+/-} clone (#653). Southern blot analysis using both 5'- and 3'-probes confirmed that both wild-type alleles had been correctly inactivated by gene targeting in the *Mus81*^{-/-} cells (Figure 1B). Northern blot analysis revealed no expression of the gene in these clones (Figure 1C). Because no additional bands were detected using the full-length *Mus81* cDNA as a probe, it is unlikely that aberrant transcripts were generated by the disruption of exon 3. The correct targeting events were confirmed by western blot analysis (Figure 1D). Levels of expression comparable to or much higher than that of endogenous expression were achieved in these mutants by the introduction of the human *Mus81* cDNA.

Generation of Eme1-deficient HCT116 cells

To compare the role of Mus81 in human cells with that of Eme1, exon 2 of *Eme1* was disrupted by a neomycin resistance gene (Figure 1E). We obtained two independent *Eme1*^{+/-} cells from 5250 neomycin-resistant colonies. *Eme1*^{-/-} cells were not successfully generated because *Eme1*^{+/-} cells grow slowly; however, *Eme1*^{+/-} cells were sufficient for the purpose of comparing the roles of these proteins. Southern and northern blot analyses confirmed the disruption of one allele of the gene (Figure 1F and G). A level of expression comparable to that of endogenous expression was achieved by the expression of human *Eme1* cDNA in *Eme1*^{+/-} cells.

Roles of the Mus81-Eme1 complex in the sensitivity to DNA damage

We next examined the sensitivity of Mus81 or Eme1 mutant cells to DNA damage by measuring their ability to form colonies following exposure to DNA-damaging agents. Because knockout cells and some complemented cells grew slowly, we took the growth rate into account in the counting of colonies (see Materials and Methods). Modest sensitivity to MMC was observed in *Mus81*^{+/-} cells (1.5-fold) and *Mus81*^{-/-} cells (4-fold) (Figure 2A). We noted a similar mild sensitivity to cisplatin in *Mus81*^{-/-} cells. Mus81 deficiency resulted in a slight sensitivity to UV radiation, MMS, hydroxyurea and ionizing radiation (Figure 2B-G). The expression of *Mus81* cDNA in *Mus81*^{-/-} cells restored the sensitivities to DNA-damaging agents to the wild-type levels. A slight increase in sensitivity to cisplatin, UV radiation and hydroxyurea was observed in *Mus81*^{+/-} cells. A similar sensitivity to MMC and hydroxyurea was found in *Eme1*^{+/-} cells. The expression of Eme1 only partially complemented the sensitivity to MMC. This is probably explained by the level of Eme1 expression in complemented cells: even if levels comparable to the endogenous levels are achieved by constitutive expression, they may not be sufficient for full complementation in response to DNA damage. Furthermore, the level of Mus81 expression is strictly dependent on the cell cycle (24), and the peak of Mus81 expression occurs in the S and G₂ phases. Like Mus81 expression, Eme1 expression may vary according to the stage of the cell cycle. These results indicate that Mus81 and Eme1 contribute to the resistance

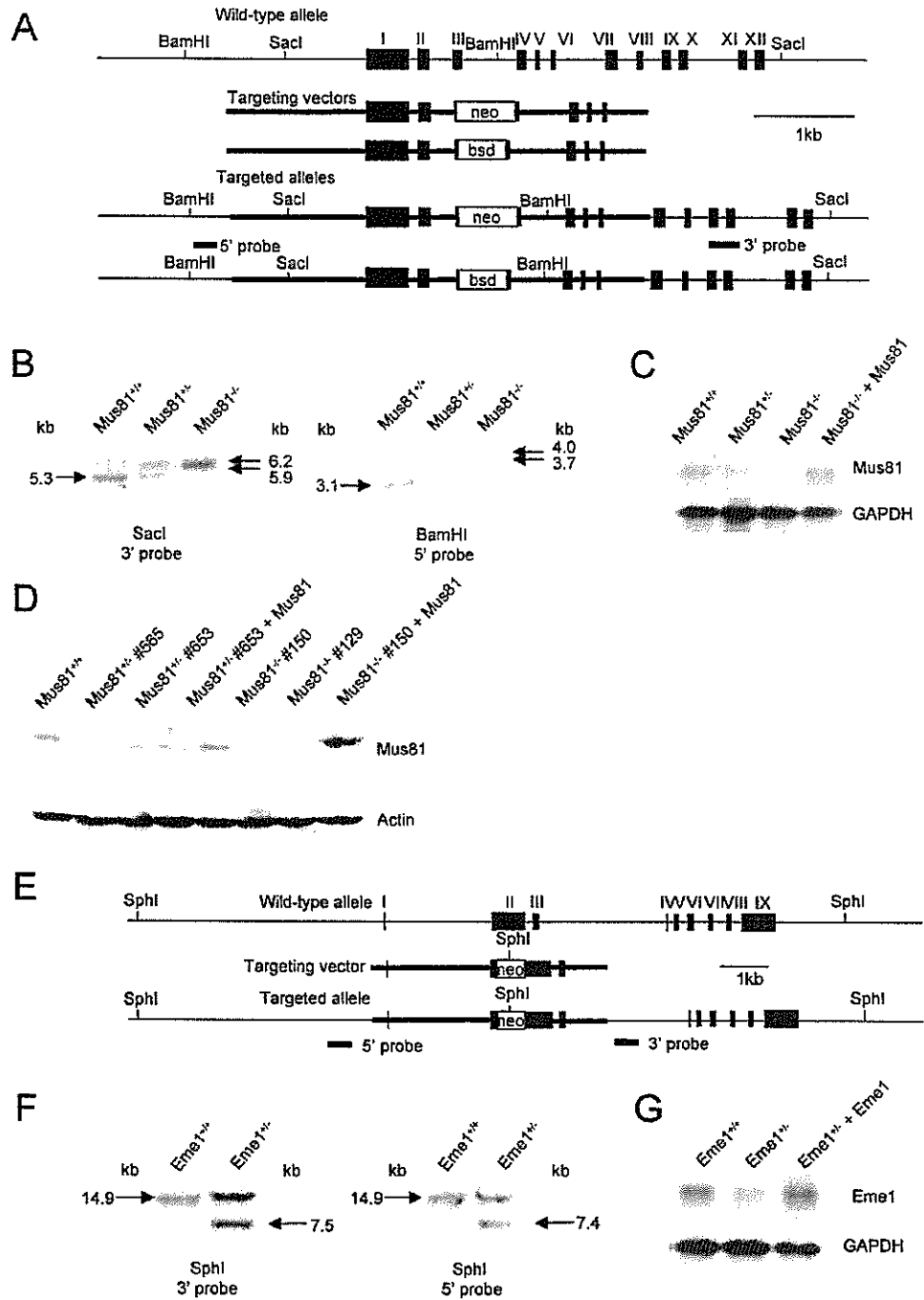


Figure 1. Generation of HCT116 cell lines deficient in *Mus81* or *Emel* by gene targeting. (A) Schematic representation of the *Mus81* locus, the targeting vectors, and the targeted alleles. Relevant restriction sites and the position of the probes used for Southern blot analysis are shown. (B) Southern blot analysis confirming targeted integration at the *Mus81* locus. DNAs were digested with *SacI* or *BamHI* and hybridized with the probes depicted in (A). (C) Northern blot analysis confirming the expression levels of *Mus81*. Poly(A)⁺ RNAs were isolated and hybridized with the full-length *Mus81* cDNA. Northern blotting for glyceraldehyde 3-phosphate dehydrogenase (GAPDH) was performed to confirm equal loading. (D) Western blot analysis confirming the protein expression levels of *Mus81*. Western blotting for actin was also carried out to confirm equal loading. (E) Schematic representation of the *Emel* locus, the targeting vector and the targeted allele. Relevant restriction sites and the position of the probes used for Southern blot analysis are shown. (F) Southern blot analysis confirming targeted integration at the *Emel* locus. DNAs were digested with *SphI* and hybridized with the probes depicted in (E). (G) Northern blot analysis confirming the expression levels of *Emel*. Poly(A)⁺ RNAs were isolated and hybridized with the full-length *Emel* cDNA.

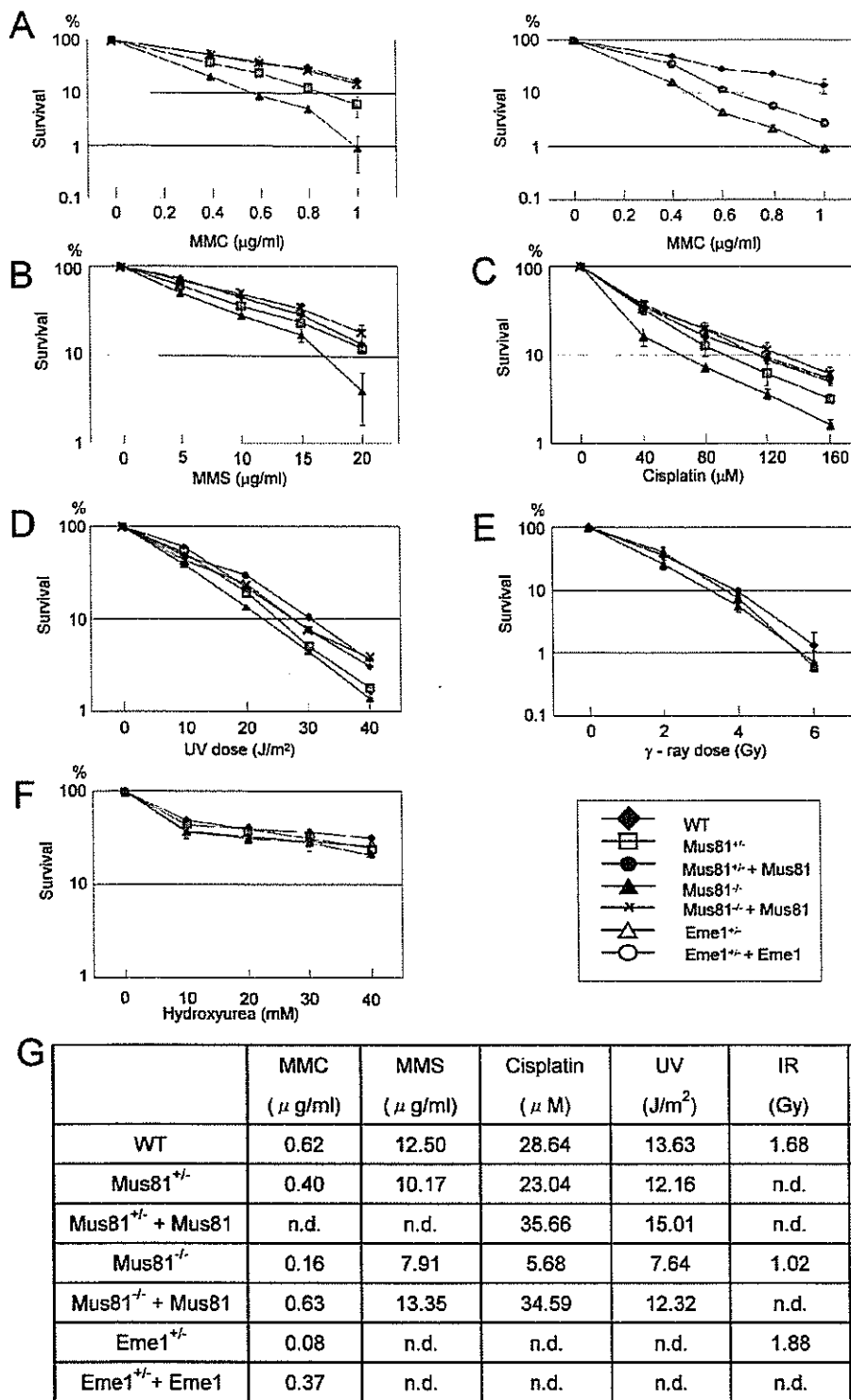


Figure 2. Sensitivity to DNA-damaging agents. (A–F) Sensitivities to MMC, MMS, cisplatin, UV radiation, ionizing radiation and hydroxyurea. Values represent the means \pm the standard error of the mean for three independent experiments. *Mus81*^{+/-} (#653), *Mus81*^{-/-} (#150) and *Eme1*^{+/-} (#376) cells were used. (G) D37 values of sensitivity to DNA-damaging agents. Graph Pad Prism4 software was used to calculate the values.

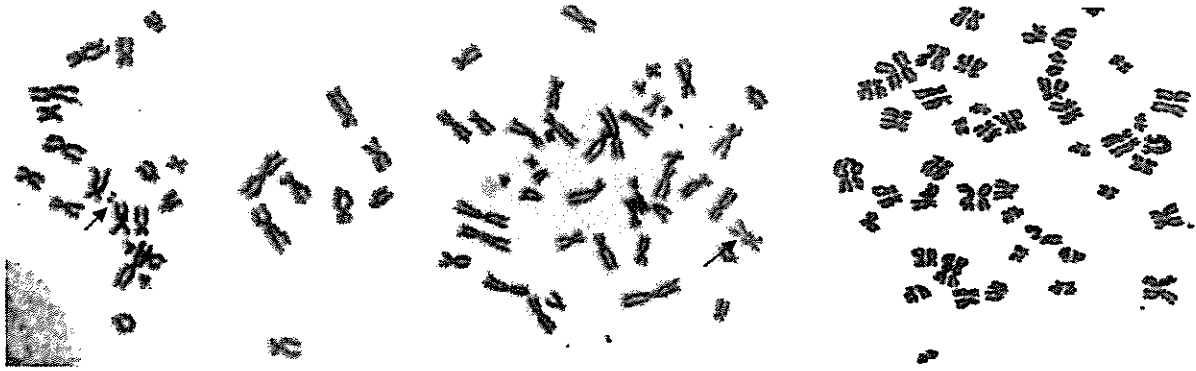


Figure 3. Chromosomal aberrations in *Mus81*^{-/-} (#150) cells. The arrow in the left panel indicates a chromosome break. The arrow in the middle panel indicates a chromatid gap. Rereplication is shown in the right panel. In the left and middle panels, only a part of metaphase chromosome image is shown.

Table 1. Chromosomal aberrations

Cell line ^a	Chromatid-type ^b (%)	Chromosome-type ^b (%)	Abnormal cells ^b (excluding tetraploidy) (%)	Tetraploidy ^c
<i>Mus81</i> ^{+/+}	2.5 ± 0.5	2.4 ± 1.1	4.5 ± 1.0	0.67% (23/3413)
<i>Mus81</i> ^{+/-}	4.9 ± 1.2	6.2 ± 1.1	10.4 ± 1.1	1.88% (39/2077)
<i>Mus81</i> ^{+/-} + <i>Mus81</i>	3.2 ± 1.6	4.5 ± 1.5	6.7 ± 0.8	0.58% (6/1041)
<i>Mus81</i> ^{-/-}	7.0 ± 1.3	10.0 ± 2.0	14.5 ± 0.5	2.46% (37/1503)
<i>Mus81</i> ^{-/-} + <i>Mus81</i>	2.4 ± 0.6	3.5 ± 1.5	5.7 ± 2.1	0.88% (27/3059)
<i>Mus81</i> ^{-/-} + <i>Cdk1</i> (#1)	6.2 ± 3.0	9.4 ± 4.1	12.9 ± 1.9	0.50% (10/2000)
<i>Mus81</i> ^{-/-} + <i>Cdk1</i> (#7)	4.0 ± 0.9	10.0 ± 0.5	11.2 ± 0.3	0.54% (6/1105)
<i>Mus81</i> ^{+/+} + <i>Cdk1</i>	2.5 ± 0.5	5.7 ± 1.6	6.9 ± 0.3	0.67% (2/300)
<i>Eme1</i> ^{+/+}	6.4 ± 1.6	6.5 ± 1.3	10.7 ± 0.3	2.16% (63/2919)
<i>Eme1</i> ^{+/-} + <i>Eme1</i>	3.5 ± 0.9	5.2 ± 1.2	7.4 ± 1.3	1.20% (15/1248)

^a*Mus81*^{+/+} (#653), *Mus81*^{-/-} (#150) and *Eme1*^{+/-} (#376) cells were used.

^bA total of 200 cells were scored for each line. Results represent the means ± SD of three independent experiments.

^cThe frequency of tetraploidy is shown as a percentage of tetraploid cells to the total number of metaphase cells analyzed; absolute numbers are given in parentheses.

of human cells to DNA-damaging agents such as DNA crosslinking agents.

Rad51 plays a central role in the early stages of homologous recombination and forms nuclear foci in a DNA damage-dependent manner (25). Impaired Rad51 focus formation has been reported in chicken and mammalian cells with defective homologous recombination (22,26,27). Rad54 plays a role in homologous recombination by dissociating Rad51 from nucleoprotein filaments formed on double-stranded DNA (28), and it forms nuclear foci that colocalize with foci of Rad51 (29). To investigate the role of Mus81 in the Rad51-dependent recombination pathway, we examined damage-dependent focus formation of Rad51 and Rad54 by treating cells with 0.8 µg/ml MMC or 8 Gy of ionizing radiation. We found no difference in focus formation between wild-type and *Mus81*^{-/-} cells (data not shown), suggesting that Mus81 is not required for focus formation by these proteins.

Mus81-Eme1 is required for chromosome stability

A defect in homologous recombination repair leads to chromosome instability (30). We examined chromosomal aberrations in the presence of colcemid using metaphase spreads. The frequency of abnormal cells harboring chromatid- and chromosome-type aberrations such as gaps and breaks

(Figure 3) was 4.5% in wild-type cells, whereas it increased to 10.4% in *Mus81*^{+/-} cells and 14.5% in *Mus81*^{-/-} cells (Table 1). Expression of the *Mus81* cDNA partially complemented these phenotypes (6.7 and 5.7%, respectively). The number of cells showing abnormalities was also increased in *Eme1*^{+/-} cells (10.7%), and it was reduced by the expression of the *Eme1* cDNA (7.4%).

In addition to these aberrations, the numbers of tetraploid cells resulting from DNA rereplication (Figure 3) were significantly increased in the mutant cells (Table 1). The frequency of tetraploidy in wild-type cells was 0.67%, whereas it increased to 1.88% (*Mus81*^{+/-}) and 2.46% (*Mus81*^{-/-}) in the mutants. Differences in frequency were statistically significant between wild-type and *Mus81*^{+/-} cells ($P < 1.0 \times 10^{-4}$) and *Mus81*^{-/-} cells ($P < 1.0 \times 10^{-6}$). The differences were statistically evaluated using multiple logistic regression analysis taking Poisson errors into account. The expression of the *Mus81* cDNA in the mutants reduced the number of tetraploid cells to a level that was comparable to wild-type cells. The frequency of tetraploid cells was also increased to 2.16% in *Eme1*^{+/-} cells ($P < 1.0 \times 10^{-5}$), and this value was reduced to 1.20% by the expression of the *Eme1* cDNA. Increases in DNA content resulting from DNA rereplication were not detected by FACS analysis, as only a small proportion of cells underwent rereplication.

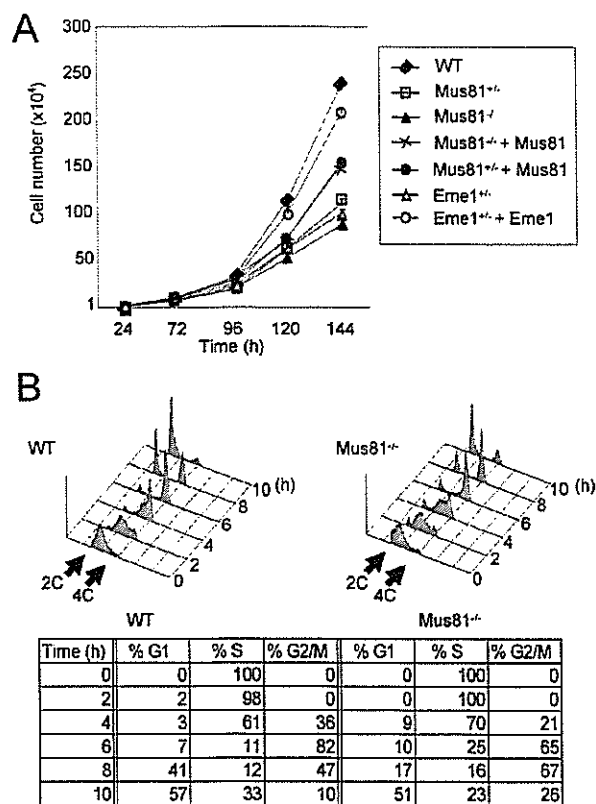


Figure 4. Effects of *Mus81* or *Eme1* deficiency on cell cycle progression. *Mus81*^{+/-} (#653), *Mus81*^{-/-} (#150) and *Eme1*^{+/-} (#376) were examined. (A) Growth curves. The results show the means \pm the standard error of the mean for three independent experiments. (B) Cell cycle distribution. The cells were synchronized in G₁/S by double-thymidine block and released. Samples were taken at the indicated time points and subjected to FACS analysis.

Mus81 or Eme1 deficiency affects cell cycle progression

The growth rates of *Mus81*^{+/-}, *Mus81*^{-/-} and *Eme1*^{+/-} cells were significantly lower than that of wild-type cells (Figure 4A). The doubling time of wild-type cells was 17 h, whereas the times for *Mus81*^{+/-}, *Mus81*^{-/-} and *Eme1*^{+/-} cells were 21, 22 and 21.5 h, respectively. Expression of the *Mus81* or *Eme1* cDNA partially complemented this phenotype. To examine the profiles of cell cycle progression, we performed FACS analysis using cells synchronized by double-thymidine block. We observed a small difference in the kinetics of accumulation of cells in the S and G₂/M phases between wild-type and *Mus81*^{-/-} cells (Figure 4B). There was a peak in G₂/M phase accumulation 6 h after release in wild-type cells, whereas G₂/M phase accumulation was found 6 and 8 h after release in *Mus81*^{-/-} cells.

Mus81 or Eme1 deficiency activates the intra-S-phase checkpoint

Cell cycle progression through S phase is regulated by cyclin E/Cdk2 and cyclin A/Cdk2. We therefore investigated the effects of *Mus81* deficiency on the S phase progression by

performing cyclin E and cyclin A kinase assays using lysates from cells synchronized in the G₁/S phase (Figure 5A). The cyclin E and cyclin A kinase activities were apparently lower in *Mus81*^{-/-} cells than in wild-type cells at 0 and 0–8 h after release, respectively. Quantitative analysis revealed that *Mus81*^{-/-} cells had a 40% reduction in cyclin E kinase activity at 0 h and a 50% reduction in cyclin A kinase activity at 4 h compared to wild-type cells. The levels of cyclin E and cyclin A in *Mus81*^{-/-} cells were almost the same as in wild-type cells at this stage of the cell cycle, indicating that S phase checkpoint activation was responsible for the reductions in cyclin kinase activities.

Because the mutant cells showed a spontaneous delay of cell cycle progression during the S phase, we first investigated the effect of *Mus81* deficiency on the ATR-Chk1 pathway, which regulates the basal turnover of Cdc25A (31). Western blot analysis using an anti-phospho-Chk1 antibody (Ser-317) revealed that levels of phospho-Chk1 were high in the early S phase and that the levels in *Mus81*^{-/-} cells were the same as in wild-type cells (Figure 5B). This finding is consistent with the proposed role of Chk1 activation in the maintenance of the physiological turnover of Cdc25A.

However, the involvement of Chk1 in a DNA damage-dependent checkpoint cannot be evaluated by this method because the basal levels of phospho-Chk1 were high during the S phase. We therefore examined the damage-dependent Chk1 activation at the single-cell level by immunofluorescence using the same antibody (Figure 5C). Clear staining in the nucleus indicating the damage-dependent phosphorylation of Chk1 on Ser-317 was observed in a small proportion of cells. This staining pattern was found in $0.3 \pm 0.1\%$ (mean \pm SD) of wild-type cells and in $1.9 \pm 0.1\%$ of *Mus81*^{-/-} cells ($n = 500$). The frequencies of the staining ranged from $0.9 \pm 0.1\%$ to $1.5 \pm 0.2\%$ in *Mus81*^{+/-} and *Eme1*^{+/-} cells.

To investigate whether ATM or ATR regulates Chk1 activation by phosphorylation in the S phase, ATM and ATR were knocked down by siRNA (Figure 5D). Silencing of ATM reduced the frequency to $0.5 \pm 0.3\%$ in *Mus81*^{-/-} cells, whereas silencing of ATR or transfection of control siRNA did not affect the frequency, indicating that the ATM-Chk1 pathway was activated in the S phase in *Mus81*^{-/-} cells (Figure 5C). This pathway has been shown to be activated in response to DSBs induced by ionizing radiation (32).

The intra-S-phase checkpoint in response to DSBs was first shown to be mediated by the ATM-Chk2-Cdc25A-Cdk2 pathway (33). Next, we investigated Chk2 activation in the S phase by immunofluorescence using an anti-phospho-Chk2 (Thr-68) antibody (Figure 5E). Phosphorylation of Chk2 on Thr-68 is required for the initiation of Chk2 activity. Clear staining of phospho-Chk2 in the nucleus was not observed in wild-type cells, but it was observed in $2.3 \pm 0.3\%$ of *Mus81*^{-/-} cells ($n = 500$). The frequency of the staining ranged from $1.0 \pm 0.2\%$ to $1.6 \pm 0.2\%$ in *Mus81*^{+/-} and *Eme1*^{+/-} cells, respectively. Silencing of ATM reduced the frequency to $0.7 \pm 0.5\%$, whereas silencing of ATR or transfection of control siRNA did not affect the frequency, indicating that ATM acted as an upstream kinase for Chk2 activation. Thus, both the ATM-Chk1 and ATM-Chk2 checkpoint pathways were activated during the S phase in the *Mus81* and *Eme1* mutant cells.

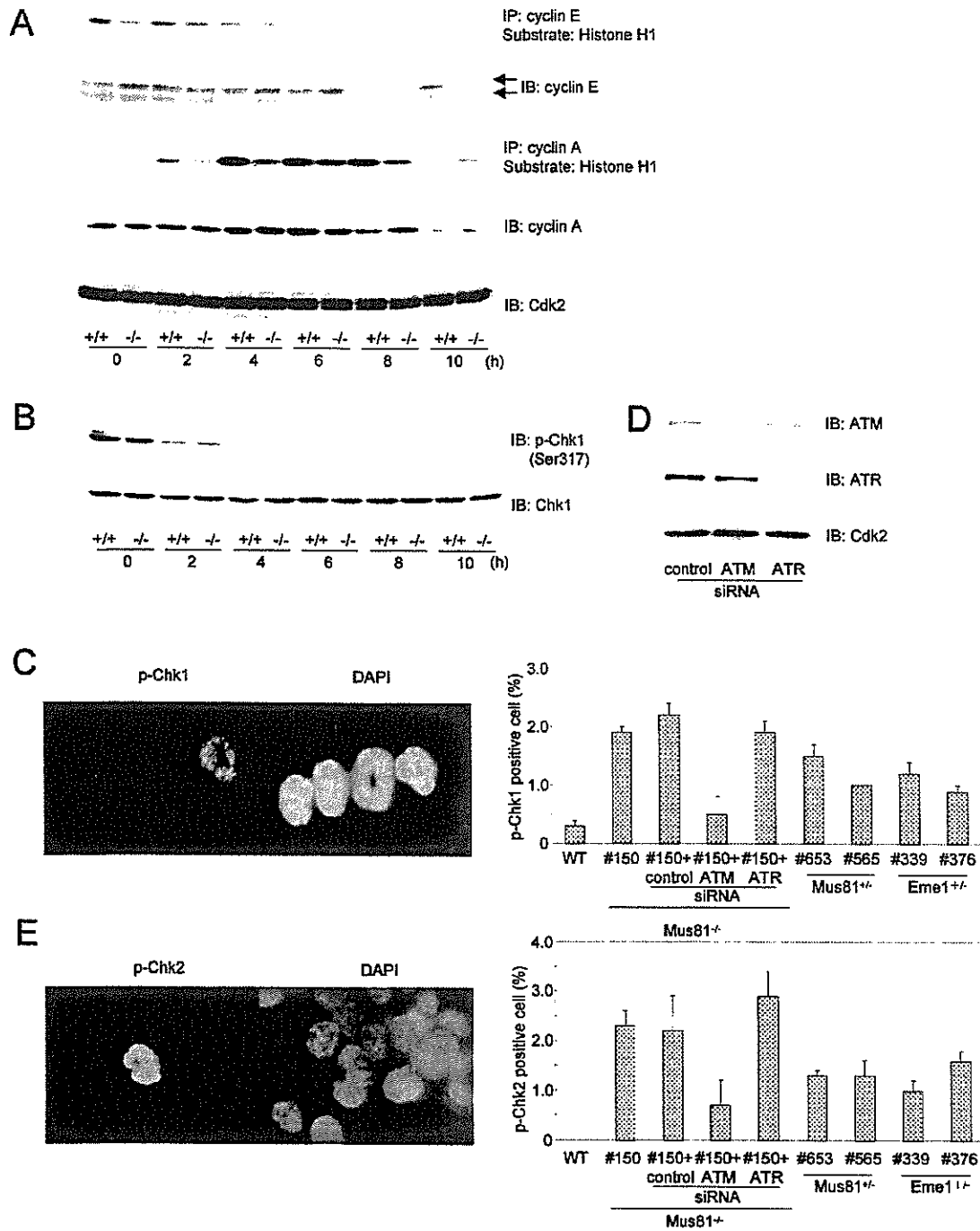


Figure 5. Activation of the intra-S-phase checkpoint. (A) Cyclin E and cyclin A kinase activities with histone H1 as the substrate. Wild-type and *Mus81*^{-/-} (#150) cells were synchronized in G₁/S by double-thymidine block and released. (B) Western blot analysis of synchronized wild-type and *Mus81*^{-/-} (#150) cell extracts using anti-phospho-Chk1 (Ser-317). The experiments in (A) and (B) were performed three times, and representative results are shown. (C) Immunofluorescence of *Mus81*^{-/-} cells synchronized in S phase using anti-phospho-Chk1 (Ser-317). The frequencies of positive staining for phospho-Chk1 are shown in the right panel. (D) Western blot analysis of unsynchronized *Mus81*^{-/-} (#150) cells transfected with siRNAs. The experiment was performed three times. (E) Immunofluorescence of *Mus81*^{-/-} cells synchronized in S phase using anti-phospho-Chk2 (Thr-68). The frequencies of the positive staining of phospho-Chk2 are shown in the right panel. In (C) and (E), cells were fixed 2 h after release, and a total of 500 cells were examined for each cell line. The results represent the means \pm standard deviation of three independent experiments. IB, immunoblot; IP, immunoprecipitation; p-Chk, phospho-Chk; WT, wild-type.

Mus81 or Eme1 deficiency activates the G₂/M checkpoint

Because FACS profiles revealed a difference in the accumulation of cells in G₂/M, we investigated the effects of Mus81 deficiency on the G₂/M delay by running a cyclin B kinase assay using cells synchronized in the G₁/S phase (Figure 6A). Cyclin B kinase activity was increased 6 h after release in wild-type cells, whereas an increase in the kinase activity was not obvious at 6 h but was clear at 8 h after release in the mutant. Repeated experiments demonstrated that such a difference between the wild-type and mutant cells could be observed either 6 or 8 h after release, consistent with the results from the FACS analysis. There were no apparent differences in cyclin B and Cdk1 levels between wild-type and *Mus81*^{-/-} cells, excluding the possibility that reduced cyclin B kinase activity was due to repression of these proteins. In addition, we noticed that the level of cyclin B expression was high even in the G₁ phase at 10 h in the HCT116 cell line. This aberrant expression of cyclin B has been observed in some human cancer cells, suggesting that it may be associated with abnormal proliferation of cancer cells (34). The high level of cyclin B may account for the sustained cyclin B kinase activity during the early G₁ phase in wild-type cells.

Activation of Cdk1 by association with cyclin B is essential for the initiation of the M phase. The delay of cyclin B activity in *Mus81*^{-/-} cells may simply indicate that the cell cycle progression was delayed by the preceding S phase delay. Alternatively, G₂/M checkpoint activation may be involved in the delay of cyclin B activity. Chk1 and Chk2 play a role in the G₂/M checkpoint as effector kinases (35). To investigate whether the G₂/M checkpoint was activated in the mutants, we therefore examined Chk1 and Chk2 kinase activities using a recombinant GST-Cdc25C (200–256) fusion protein as a substrate. These kinases preferentially phosphorylate Cdc25C on Ser-216 (36). We examined the difference in Chk2 kinase activity in synchronized cells. Chk2 kinase activity was significantly increased in the *Mus81* mutant 6 h after release, whereas an increase was not evident in wild-type cells (Figure 6B). There were no differences in the levels of Chk2. A more than 3-fold increase in Chk2 activity was also observed in two *Mus81*^{+/-} cell lines as well as in two *Eme1*^{+/-} cell lines, excluding the possibility that activation of Chk2 was due to a clonal variation (Figure 6C). Expression of *Mus81* or *Eme1* cDNA reduced this increase in Chk2 activity in the mutant cells (Figure 6C). Chk2 kinase phosphorylation of Cdc25C was not clearly observed before 6 h, indicating that the increase in this activity at 6 h reflected the G₂/M checkpoint activation rather than a delay of the cell cycle progression. The S phase checkpoint was activated in *Mus81*^{-/-} cells from 0 to 4 h after release.

The increase in Chk2 kinase activity was abolished in the presence of 0.5 mM caffeine (Figure 6C). Treatment with 0.5 mM caffeine for 1 h has little effect on DNA synthesis (37), excluding the possibility that the elimination of Chk2 activity by caffeine was due to the delay in cell cycle progression. Because caffeine inhibits ATM and ATR kinase activities (38–40), they are likely required for this increase in Chk2 kinase activity. For this reason, we further investigated the effect of siRNA silencing of ATM and ATR on Chk2 activity (Figures 5D and 6D). Chk2 activity was reduced by silencing

of ATM but not by silencing of ATR, indicating that the activation of ATM in response to DNA damage is responsible for the increase in Chk2 activity in *Mus81*^{-/-} cells. In contrast, there was no clear difference in the phosphorylation of GST-Cdc25C (200–256) by Chk1 in wild-type and *Mus81*^{-/-} cells (Figure 6E). There was also no difference in p21 expression in wild-type and *Mus81*^{-/-} cells (Figure 6F).

It is assumed that the p21-dependent G₂/M checkpoint leads to sustained cell cycle arrest, whereas the Cdc25-dependent checkpoint leads to transient delay (41). Consistent with this idea, many delayed cells eventually proceeded into the M and G₁ phases. These results show that, in addition to the intra-S-phase checkpoint, the G₂/M checkpoint was activated in the *Mus81* mutant cells via the ATM-Chk2 pathway.

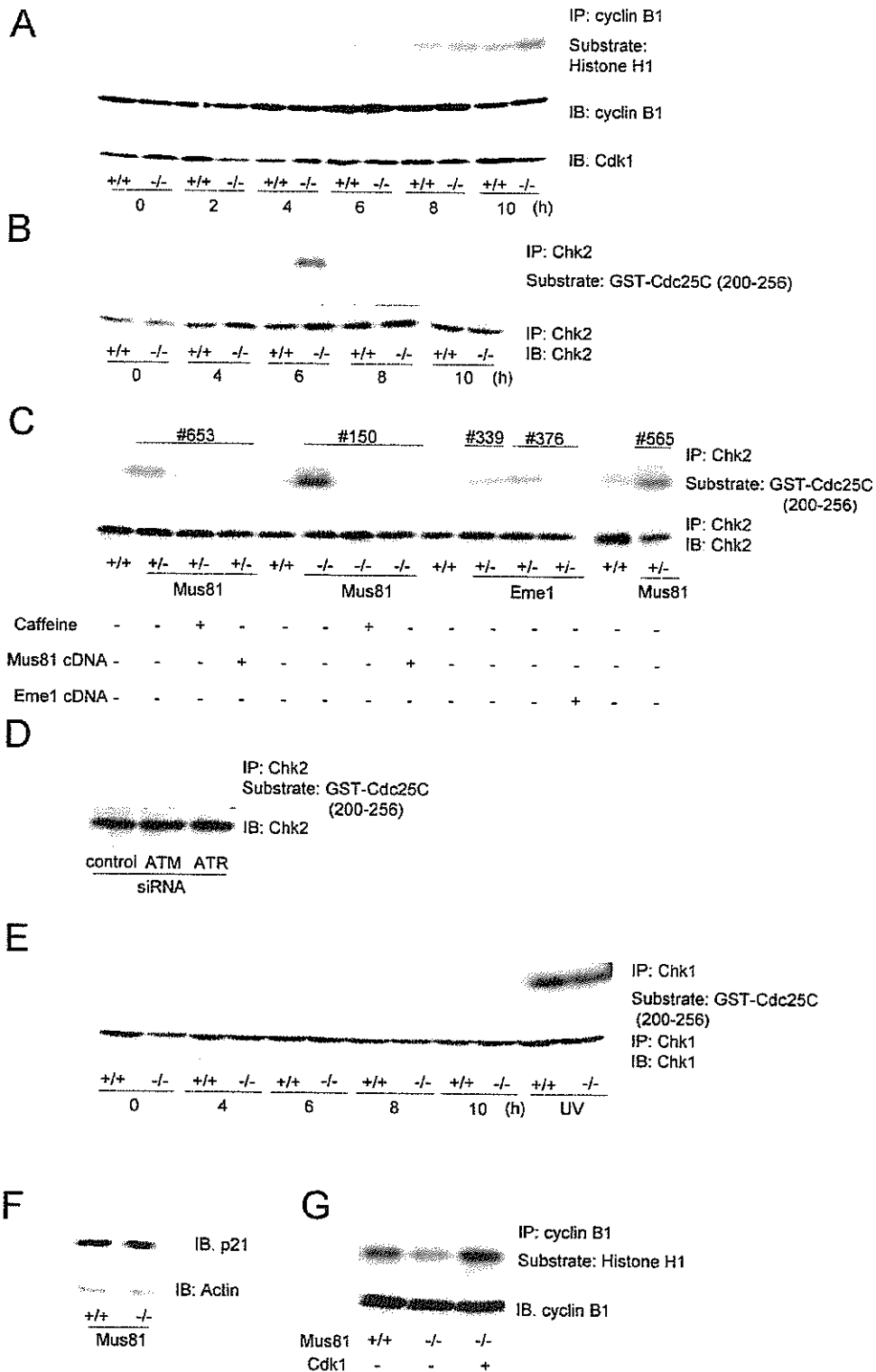
Overexpression of Cdk1 prevents rereplication

Because deletion of Cdk1 promotes DNA rereplication in human cells (42), reduced cyclin B kinase activity is likely to cause increased rereplication in *Mus81* mutants. We examined this possibility by overexpressing Cdk1 in the *Mus81* mutants. Cdk1 kinase activity is regulated by accumulation of Cdk1-associated cyclin B and removal of inhibitory protein phosphorylations. Western blot analysis revealed that levels of cyclin B were high in G₂/M in *Mus81*^{-/-} cells while the levels of Cdk1 were constant, suggesting that overexpressed Cdk1 may be associated with endogenous cyclin B. Given that overexpressed Cdk1 is not phosphorylated on inhibitory phosphorylation sites by overcoming Wee1 and Myt1 kinase activities, Cdk1 activity is expected to be increased. Because we showed that p21 is not induced in *Mus81*^{-/-}, it is not necessary to consider direct inhibition of Cdk2 activity by p21. Consistent with this hypothesis, the reduction of cyclin B kinase activity was reversed by the overexpression of Cdk1 (Figure 6G). The increase in cyclin B activity by ectopic expression of Cdk1 reduced the frequency of tetraploidy from 2.46 to 0.50% and 0.54% in the two *Mus81*^{-/-} cell lines ($P < 1.0 \times 10^{-2}$) (Table 1). Thus, the increased rereplication in *Mus81* mutants was reversed by ectopic expression of Cdk1.

DISCUSSION

In the current studies, we demonstrated that *Mus81*–*Eme1* deficiency activates the intra-S-phase and G₂/M checkpoints in response to DNA damage and promotes DNA rereplication. In addition, we confirmed that the *Mus81*–*Eme1* complex contributes to the resistance against DNA-damaging agents in human cells. These assays show quite small differences, suggesting that there may be functional redundancy between the *Mus81*–*Eme1* complex and other repair proteins in the response to DNA damage. Consistent with extensive genetic studies in yeast, the results of the present study indicate that there is no functional difference between *Mus81* and *Eme1* in human cells.

Identification of the physiological substrates of the *Mus81*–*Eme1* complex has long remained elusive. However, a study showing the presence of resolvase activities in two separate fractions from human cell extracts has significantly enhanced our understanding of this complex system (43,44). The *Mus81*–*Eme1* complex shows a greater activity for the



3'-flap and three-way branched fork structures, whereas the Rad51C complex shows specific activity for Holliday junctions. These findings suggest that replication forks or 3'-flaps may be the *in vivo* substrates of the Mus81 endonuclease. The present finding that the Mus81–Eme1 complex confers resistance to DNA crosslinking agents, MMS and hydroxyurea supports this idea because these agents cause stalled replication forks. However, it is also possible that recombination intermediates such as D-loops and Holliday junctions are the *in vivo* substrates of the endonuclease. This possibility is supported by the observation that mutations in genes such as *RAD51*, *RAD52*, *RAD55* and *RAD57* that play early roles in recombination suppress the synthetic lethality of *mus81* (or *mms4*) *sgs1* (or *top3*) mutants (45,46). If Mus81–Mms4 directly cleaves replication forks and does not play a late role, synthetic lethality would not be rescued by a defect in these genes. The physical interaction of Mus81 with Rad54 in yeast is consistent with this idea (5). Furthermore, Mus81 has been shown to play a key role in the Rhp51-independent recombination repair pathway in fission yeast by resolving D-loops formed by Rad22 (47).

We observed spontaneous activation of the intra-S-phase checkpoint through two independent cascades in *Mus81*^{-/-} cells. The ATM-Chk2-Cdc25A-Cdk2 pathway has been shown to play a role in the intra-S-phase checkpoint in response to DSBs. In addition, the damage-dependent Chk1 pathway was activated by ATM but not by ATR. This finding strongly suggests that the Mus81–Eme1 complex is involved in the processing of DSBs. This notion is also supported by the present finding that Mus81 or Eme1 deficiency led to the activation of the G₂/M checkpoint through the ATM-Chk2 pathway. DSBs that escape the intra-S-phase checkpoint and/or DSBs generated in G₂ can activate the G₂/M checkpoint. Thus, the recombination intermediates are likely to be the *in vivo* target of the Mus81–Eme1 complex. It is also possible that stalled replication forks, if unprocessed, generate DSBs, which could activate the ATM-dependent checkpoint pathway. In contrast to ATM, ATR kinase activity is activated by several kinds of DNA damage, including those caused by UV radiation and chemicals that make bulky base lesions, as well as by stalled replication forks (48). Although the present study demonstrated that Chk1 is not activated by ATR, it is very likely that ATR was activated in *Mus81*^{-/-} cells. Despite the fact that cyclin A activity was strongly repressed, activation of Chk1 and Chk2 could account for the S phase delay only in a small proportion of the Mus81 and Eme1 mutant cells. In addition to the intra-S-phase checkpoint, the replication checkpoint initiated by ATR is likely to play a major role in the S phase delay resulting from Mus81 or Eme1 deficiency. Identification of the effectors that protect the replication fork will address this issue.

Mus81 has been shown to be physically associated with Cds1 (Chk2) in yeast and in human cells, suggesting a functional link between these proteins. We found that ionizing radiation- or MMC-induced phosphorylation of Chk2 on Thr-68 is not affected by a deficiency of Mus81 (data not shown), suggesting that Mus81 does not directly regulate the function of Chk2. Conversely, phosphorylation of Mus81 by Chk2 has been shown to be required for the maintenance of genome integrity during replication stress (19).

Evidence for the molecular mechanisms underlying checkpoint activation in response to DNA damage has largely come from studies in cells exposed to DNA-damaging agents. In contrast to these studies, our results provide new insight into the mechanism of checkpoint activation in response to DNA damage that spontaneously arises from a defect in a single process of DNA repair where there is no exogenous DNA damage. Reactive cellular metabolites are assumed to become endogenous genotoxic insults. Because the cells were more sensitive to DNA crosslinking agents than other agents, it is of interest to identify the sources of endogenous DNA interstrand crosslinks.

In addition to increased chromosomal aberrations such as gaps and breaks, we found increased frequencies of tetraploidy in the Mus81–Eme1 mutants. In yeast, B-type cyclin-dependent kinases prevent rereplication by several overlapping mechanisms, including phosphorylation of ORC, down-regulation of Cdc6 and nuclear exclusion of MCM proteins (49). The ability of these kinases to prevent rereplication is also supported by the finding that cyclin B/Cdk1 is associated with replication origins (50). In human cells, deletion of Cdk1 by gene targeting results in increased levels of tetraploidy (42). It is therefore likely that reduced cyclin B/Cdk1 kinase activity caused increased rereplication in the Mus81 mutants. This model is supported by our finding that the overexpression of Cdk1 prevents rereplication in Mus81 mutants, although we cannot exclude the possibility that Cdk1 overexpression plays an indirect role in preventing rereplication. Chromosomes in tetraploid cells are very unstable, as demonstrated by the finding that tetraploid-derived mouse tumors have numerical and structural chromosomal aberrations (51). The aneuploidy observed in mouse *Mus81*^{-/-} cells may result from chromosome instability in tetraploid cells. Recent evidence has suggested that aneuploid cells proceed through a tetraploid state (52). This possibility may also account for the absence of a clear peak of 8C DNA content in *Mus81*^{-/-} cells in FACS profiles. We observed extremely low frequency of DNA contents ranging from 4C to 8C at high magnification, which apparently concealed a small peak at 8C.

Haploinsufficiency of *Mus81* was found to cause phenotypes similar to those of a complete loss of the gene. Similar results were observed for *Mus81*^{+/-} and *Mus81*^{-/-} mice. Loss

Figure 6. Activation of the G₂/M checkpoint. (A) Cyclin B kinase activity with histone H1 as the substrate. Wild-type and *Mus81*^{-/-} (#150) cells were synchronized in G₁/S by double-thymidine block and released. (B) Chk2 kinase activity using GST-Cdc25C (200–256) as the substrate and whole-cell extracts from wild-type and *Mus81*^{-/-} (#150) cells synchronized in G₁/S and released. The experiments in (A) and (B) were performed five times. (C) Chk2 kinase activity on GST-Cdc25C (200–256) of synchronized cells harvested 6 h after release. For caffeine treatment, cells were incubated in the presence of 0.5 mM caffeine for 1 h prior to cell lysis. (D) The effects of ATM and ATR on Chk2 activity. Shown is the Chk2 kinase activity using GST-Cdc25C (200–256) as a substrate in extracts of *Mus81*^{-/-} (#150) cells harvested 48 h after transfection with siRNA. (E) Chk1 kinase activity using GST-Cdc25C (200–256) as a substrate in extracts from wild-type and *Mus81*^{-/-} (#150) cells synchronized in G₁/S and released. Cells treated with UV radiation are used as positive controls. The treated cells were harvested 5 h after UV radiation (40 J/m²). The experiments in (C), (D) and (E) were performed twice, and representative results are shown. (F) Western blot analysis of extracts from unsynchronized cells using an anti-p21 antibody. (G) Cyclin B kinase activity with histone H1 as a substrate in extracts from unsynchronized cells. In (F) and (G), *Mus81*^{-/-} (#150) cells were used.

of heterozygosity is commonly observed in tumors. The human *Mus81* gene maps to chromosome 11q13.1. Although loss of heterozygosity at the *Mus81* locus in tumors has not been reported, normal or precancerous cells have a chance to lose one allele of *Mus81*. Given that cells lose one copy of *Mus81* during tumor progression, aberrant replication fork structures and recombination intermediates are expected to accumulate and eventually lead to further genomic instability. Haploinsufficiency of *Mus81* may contribute to tumor progression through this mechanism. It is noteworthy that predisposition to cancer was not observed over 15 months in another *Mus81*^{-/-} mouse model (7). This discrepancy may be explained by a difference in strains. However, it is most likely that *Mus81* deficiency does not directly contribute to tumor formation but rather induces chromosome aberrations such as aneuploidy that do not directly lead to cancer. A long latency, during which chromosomal aberrations accumulate, may be required for tumor formation in such a situation. It is also possible that additional modifiers that promote different types of genomic instability are required for tumor formation.

The present finding that small changes in the gene dosage of *Mus81*-*Eme1* promote rereplication implicates the significance of small amounts of genotoxic insults in chromosome stability. Even in the absence of exogenous genotoxic sources, endogenous insults can lead to chromosome instability by damaging DNA. Aberrant fork structures and recombination intermediates are expected to accumulate in cells exposed to genotoxic insults. These cells suffer from increased rereplication in response to DNA damage, which does not immediately lead to tumor-associated genomic aberrations. Instead, this pathway can contribute to tumor development by inducing centrosome dysfunction and aneuploidy after numerous rounds of the cell cycle. This scenario may explain cases of radiation-induced carcinogenesis in which patients develop tumors after long periods of exposure to low-dose radiation.

ACKNOWLEDGEMENTS

The authors would like to thank M. Ohtaki for statistical analyses. The authors also thank A. Shinohara for providing the anti-Rad51 and anti-Rad54 antibodies. This work was supported by the Ministry of Education, Culture, Sports, Science and Technology and by the Ministry of Health, Labor and Welfare of Japan. M.K. and T.Y. were supported by the Hiroshima University 21st Century COE Program. Funding to pay the Open Access publication charges for this article was provided by the Ministry of Education, Culture, Sports, Science and Technology of Japan.

Conflict of interest statement. None declared.

REFERENCES

- Branzei, D. and Foiani, M. (2005) The DNA damage response during DNA replication. *Curr. Opin. Cell Biol.*, **17**, 568–575.
- Sancar, A., Lindsey-Boltz, L.A., Unsal-Kacmaz, K. and Linn, S. (2004) Molecular mechanisms of mammalian DNA repair and the DNA damage checkpoints. *Annu. Rev. Biochem.*, **73**, 39–85.
- Lambert, S., Watson, A., Sheedy, D.M., Martin, B. and Carr, A.M. (2005) Gross chromosomal rearrangements and elevated recombination at an inducible site-specific replication fork barrier. *Cell*, **121**, 689–702.
- Boddy, M.N., Lopez-Girona, A., Shanahan, P., Interthal, H., Heyer, W.-D. and Russell, P. (2000) Damage tolerance protein *Mus81* associates with the *FHA1* domain of checkpoint kinase *Cds1*. *Mol. Cell Biol.*, **20**, 8758–8766.
- Interthal, H. and Heyer, H.-D. (2000) *MUS81* encodes a novel Helix-hairpin-Helix protein involved in the response to UV- and methylation-induced DNA damage in *Saccharomyces cerevisiae*. *Mol. Gen. Genet.*, **263**, 812–827.
- Doe, C.L., Ahn, J.S., Dixon, J. and Whitby, M.C. (2002) *Mus81*-*Eme1* and *Rqh1* involvement in processing stalled and collapsed replication forks. *J. Biol. Chem.*, **277**, 32753–32759.
- Dendouga, N., Gao, H., Moechars, D., Janicot, M., Vialard, J. and McGowan, C.H. (2005) Disruption of murine *Mus81* increases genomic instability and DNA damage sensitivity but does not promote tumorigenesis. *Mol. Cell Biol.*, **25**, 7569–7579.
- Kalliraman, V., Mullen, J.R., Fricke, W.M., Bastin-Shanower, S.A. and Brill, S.J. (2001) Functional overlap between *Sgs1*-*Top3* and the *Mms4*-*Mus81* endonuclease. *Genes Dev.*, **15**, 2730–2740.
- Boddy, M.N., Gaillard, P.-H.L., McDonald, W.H., Shanahan, P., Yates, J.R., III and Russell, P. (2001) *Mus81*-*Eme1* are essential components of a Holliday junction resolvase. *Cell*, **107**, 537–548.
- Abraham, J., Lemmers, B., Hande, M.P., Moynahan, M.E., Chahwan, C., Ciccio, A., Essers, J., Hanada, K., Chahwan, R., Khaw, A.K. et al. (2003) *Eme1* is involved in DNA damage processing and maintenance of genomic stability in mammalian cells. *EMBO J.*, **22**, 6137–6147.
- Blais, V., Gao, H., Elwell, C.A., Boddy, M.N., Gaillard, P.-H.L., Russell, P. and McGowan, C.H. (2004) RNA interference inhibition of *Mus81* reduces mitotic recombination in human cells. *Mol. Biol. Cell*, **15**, 552–562.
- Ciccio, A., Constantinou, A. and West, S.C. (2003) Identification and characterization of the human *Mus81*-*Eme1* endonuclease. *J. Biol. Chem.*, **278**, 25172–25178.
- Ogrunc, M. and Sancar, A. (2003) Identification and characterization of human *MUS81*-*MMS4* structure specific endonuclease. *J. Biol. Chem.*, **278**, 21715–21720.
- Chen, X.-B., Melchionna, R., Denis, C.-M., Gaillard, P.-H.L., Blasina, A., Van de Weyer, I., Boddy, M.N., Russell, P., Vialard, J. and McGowan, C.H. (2001) Human *Mus81*-associated endonuclease cleaves Holliday junctions *in vitro*. *Mol. Cell*, **8**, 1117–1127.
- Gaillard, P.-H.L., Noguchi, E., Shanahan, P. and Russell, P. (2003) The endogenous *Mus81*-*Eme1* complex resolves Holliday junctions by a nick and counternick mechanism. *Mol. Cell*, **12**, 747–759.
- Osman, F., Dixon, J., Doe, C.L. and Whitby, M.C. (2003) Generating crossovers by resolution of nicked Holliday junctions: a role for *Mus81*-*Eme1* in meiosis. *Mol. Cell*, **12**, 761–774.
- de los Santos, T., Loidl, J., Larkin, B. and Hollingsworth, N.M. (2001) A role for *MMS4* in the processing of recombination intermediates during meiosis in *Saccharomyces cerevisiae*. *Genetics*, **159**, 1511–1525.
- McPherson, J.P., Lemmers, B., Chahwan, R., Pamidi, A., Migon, E., Matysiak-Zablock, E., Moynahan, M.E., Essers, J., Hanada, K., Poonepalli, A. et al. (2004) Involvement of mammalian *Mus81* in genome integrity and tumor suppression. *Science*, **304**, 1822–1826.
- Kai, M., Boddy, M.N., Russell, P. and Wang, T.S.-F. (2005) Replication checkpoint kinase *Cds1* regulates *Mus81* to preserve genome integrity during replication stress. *Genes Dev.*, **19**, 919–932.
- Michel, L.S., Liberal, V., Chatterjee, A., Kirchweger, R., Pasche, B., Gerald, W., Dobles, M., Sorger, P.K., Murty, V.V. and Benzra, R. (2001) *MAD2* haplo-insufficiency causes premature anaphase and chromosome instability in mammalian cells. *Nature*, **409**, 355–359.
- Miyagawa, K., Tsuruga, T., Kinomura, A., Usui, K., Katsura, M., Tashiro, S., Mishima, H. and Tanaka, K. (2002) A role for *RAD54B* in homologous recombination in human cells. *EMBO J.*, **21**, 175–180.
- Yoshihara, T., Ishida, M., Kinomura, A., Katsura, M., Tsuruga, T., Tashiro, S., Asahara, T. and Miyagawa, K. (2004) *XRCC3* deficiency results in a defect in recombination and increased endoreduplication in human cells. *EMBO J.*, **23**, 670–680.
- Wassmann, K. and Benzra, R. (1998) *Mad2* transiently associates with an APC/p55Cdc complex during mitosis. *Proc. Natl. Acad. Sci. USA*, **95**, 11193–11198.
- Gao, H., Chen, X.-B. and McGowan, C.H. (2003) *Mus81* endonuclease localizes to nucleoli and to regions of DNA damage in human S phase cells. *Mol. Biol. Cell*, **14**, 4826–4834.
- Tashiro, S., Walter, J., Shinohara, A., Kamada, N. and Cremer, T. (2000) *Rad51* accumulation at sites of DNA damage and in postreplicative chromatin. *J. Cell Biol.*, **150**, 283–291.

26. Bishop, D.K., Ear, U., Bhattacharyya, A., Calderone, C., Beckett, M., Weichselbaum, R.R. and Shinohara, A. (1998) Xrcc3 is required for assembly of Rad51 complexes *in vivo*. *J. Biol. Chem.*, **273**, 21482–21488.
27. Takata, M., Sasaki, M.S., Tachiiri, S., Fukushima, T., Sonoda, E., Schild, D., Thompson, L.H. and Takeda, S. (2001) Chromosome instability and defective recombinational repair in knockout mutants of the five Rad51 paralogs. *Mol. Cell. Biol.*, **21**, 2858–2866.
28. Solinger, J.A., Kitanitsa, K. and Heyer, W.-D. (2002) Rad54, a Swi2/Snf2-like recombinational repair protein, disassembles Rad51:dsDNA filaments. *Mol. Cell*, **10**, 1175–1188.
29. Tan, T.L.R., Essers, J., Citterio, E., Swagemakers, S.M.A., de Wit, J., Benson, F.E., Hoeijmakers, J.H.J. and Kanaar, R. (1999) Mouse Rad54 affects DNA conformation and DNA-damage-induced Rad51 foci formation. *Curr. Biol.*, **9**, 325–328.
30. Thompson, L.H. and Schild, D. (2001) Homologous recombinational repair of DNA ensures mammalian chromosome stability. *Mutat. Res.*, **477**, 131–153.
31. Bartek, J., Lukas, C. and Lukas, J. (2004) Checking on DNA damage in S phase. *Nature Rev. Mol. Cell Biol.*, **5**, 792–804.
32. Sorensen, C.S., Syljuasen, R.G., Falck, J., Schroeder, T., Ronnstrand, L., Khanna, K.K., Zhou, B.-B., Bartek, J. and Lukas, J. (2003) Chk1 regulates the S phase checkpoint by coupling the physiological turnover and ionizing radiation-induced accelerated proteolysis of Cdc25A. *Cancer Cell*, **3**, 247–258.
33. Falck, J., Mailand, N., Syljuasen, R.G., Bartek, J. and Lukas, J. (2001) The ATM-Chk2-Cdc25A checkpoint pathway guards against radioresistant DNA synthesis. *Nature*, **410**, 842–847.
34. Shen, M., Feng, Y., Gao, C., Tao, D., Hu, J., Reed, E., Li, Q.Q. and Gong, J. (2004) Detection of cyclin B1 expression in G₁ phase cancer cell lines and cancer tissues by postsorting western blot analysis. *Cancer Res.*, **64**, 1607–1610.
35. Iliakis, G., Wang, Y., Guan, J. and Wang, H. (2003) DNA damage checkpoint control in cells exposed to ionizing radiation. *Oncogene*, **22**, 5834–5847.
36. Matsuoka, S., Huang, M. and Elledge, S.J. (1998) Linkage of ATM to cell cycle regulation by the Chk2 protein kinase. *Science*, **282**, 1893–1897.
37. Kaufmann, W.K., Heffernan, T.P., Beaulieu, L.M., Doherty, S., Frank, A.R., Zhou, Y., Bryant, M.F., Zhou, T., Luche, D.D., Nikolaishvili-Feinberg, N. *et al.* (2003) Caffeine and human DNA metabolism: the magic and the mystery. *Mutat. Res.*, **532**, 85–102.
38. Blasina, A., Price, B.D., Turenne, G.A. and McGowan, C.H. (1999) Caffeine inhibits the checkpoint kinase ATM. *Curr. Biol.*, **9**, 1135–1138.
39. Sarkaria, J.N., Busby, E.C., Tibbetts, R.S., Roos, P., Taya, Y., Karnitz, L.M. and Abraham, R.T. (1999) Inhibition of ATM and ATR kinase activities by the radiosensitizing agent, caffeine. *Cancer Res.*, **59**, 4375–4382.
40. Zhou, B.-B.S., Chaturvedi, P., Spring, K., Scott, S.P., Johanson, R.A., Mishra, R., Mattern, M.R., Winkler, J.D. and Khanna, K.K. (2000) Caffeine abolishes the mammalian G₂/M DNA damage checkpoint by inhibiting ataxia-telangiectasia-mutated kinase activity. *J. Biol. Chem.*, **275**, 10342–10348.
41. Lukas, J., Lukas, C. and Bartek, J. (2004) Mammalian cell cycle checkpoints: signaling pathways and their organization in space and time. *DNA Repair*, **3**, 997–1007.
42. Itzhaki, J.E., Gilbert, C.S. and Porter, A.C.G. (1997) Construction by gene targeting in human cells of a 'conditional' *CDC2* mutant that rereplicates its DNA. *Nature Genet.*, **15**, 258–265.
43. Constantinou, A., Chen, X.-B., McGowan, C.H. and West, S.C. (2002) Holliday junction resolution in human cells: two junction endonucleases with distinct substrate specificities. *EMBO J.*, **21**, 5577–5585.
44. Liu, Y., Masson, J.-Y., Shah, R., O'Regan, P. and West, S.C. (2004) RAD51C is required for Holliday junction processing in mammalian cells. *Science*, **303**, 243–246.
45. Bastin-Shanower, S.A., Fricke, W.M., Mullen, J.R. and Brill, S.J. (2003) The mechanism of Mus81-Mms4 cleavage site selection distinguishes it from the homologous endonuclease Rad1-Rad10. *Mol. Cell. Biol.*, **23**, 3487–3496.
46. Fabre, F., Chan, A., Heyer, W.-D. and Gangloff, S. (2002) Alternate pathways involving Sgs1/Top3, Mus81/Mms4, and Srs2 prevent formation of toxic recombination intermediates from single-stranded gaps created by DNA replication. *Proc. Natl Acad. Sci. USA*, **99**, 16887–16892.
47. Doe, C.L., Osman, F., Dixon, J. and Whitby, M.C. (2004) DNA repair by a Rad22-Mus81-dependent pathway that is independent of Rhp51. *Nucleic Acids Res.*, **32**, 5570–5581.
48. Abraham, R.T. (2001) Cell cycle checkpoint signaling through the ATM and ATR kinases. *Genes Dev.*, **15**, 2177–2196.
49. Nguyen, V.Q., Co, C. and Li, J.J. (2001) Cyclin-dependent kinases prevent DNA re-replication through multiple mechanisms. *Nature*, **411**, 1068–1073.
50. Wuarin, J., Buck, V., Nurse, P. and Millar, J.B.A. (2002) Stable association of mitotic Cyclin B/Cdc2 to replication origins prevents endoreduplication. *Cell*, **111**, 419–431.
51. Fujiwara, T., Bandi, M., Nitta, M., Ivanova, E.V., Bronson, R.T. and Pellman, D. (2005) Cytokinesis failure generating tetraploids promotes tumorigenesis in *p53*-null cells. *Nature*, **437**, 1043–1047.
52. Shi, Q. and King, R.W. (2005) Chromosome nondisjunction yields tetraploid rather than aneuploid cells in human cell lines. *Nature*, **437**, 1038–1042.



Src tyrosine kinase inhibitor PP2 suppresses ERK1/2 activation and epidermal growth factor receptor transactivation by X-irradiation

Zhiping Li^a, Yoshio Hosoi^{a,*}, Keshong Cai^a, Yuji Tanno^a, Yoshihisa Matsumoto^a, Atsushi Enomoto^a, Akinori Morita^a, Keiichi Nakagawa^b, Kiyoshi Miyagawa^a

^a Department of Radiation Research, Faculty of Medicine, University of Tokyo, Tokyo 113-0033, Japan

^b Department of Radiology, Faculty of Medicine, University of Tokyo, Tokyo 113-0033, Japan

Received 26 December 2005

Available online 18 January 2006

Abstract

Exposure of MDA-MB-468 cells to ionizing radiation (IR) caused biphasic activation of ERK as indicated by its phosphorylation at Thr202/Tyr204. Specific epidermal growth factor receptor (EGFR) inhibitor AG1478 and specific Src inhibitor PP2 inhibited IR-induced ERK1/2 activation but phosphatidylinositol-3 kinase inhibitor wortmannin did not. IR caused EGFR tyrosine phosphorylation, whereas it did not induce EGFR autophosphorylation at Tyr992, Tyr1045, and Tyr1068 or Src-dependent EGFR phosphorylation at Tyr845. SHP-2, which positively regulates EGFR/Ras/ERK signaling cascade, became activated by IR as indicated by its phosphorylation at Tyr542. This activation was inhibited by PP2 not by AG1478, which suggests Src-dependent activation of SHP-2. Src and PTP α , which positively regulates Src, became activated as indicated by phosphorylation at Tyr416 and Tyr789, respectively. These data suggest that IR-induced ERK1/2 activation involves EGFR through a Src-dependent pathway that is distinct from EGFR ligand activation. © 2006 Elsevier Inc. All rights reserved.

Keywords: Ionizing radiation; EGFR; Src; Transactivation; ERK; SHP-2; PP2; AG1478

Ionizing radiation (IR) has been shown to activate epidermal growth factor receptor (EGFR) and extracellular signal-regulated kinase (ERK) [1–3]. EGFR activation by IR initiates the Ras/Raf/ERK signaling cascade, stimulates cell proliferation, and leads cells to be resistant to IR [1–5]. The molecular mechanisms underlying IR-induced activation of EGFR are not clear. One of the possible mechanisms is activation of Src. IR induces production of hydrogen peroxide. Treatment with hydrogen peroxide activates Src, and specific EGFR inhibitor AG1478, and specific Src inhibitors PP1 and PP2 inhibit the activation of EGFR and ERK1/2 induced by hydrogen peroxide [6–9]. Ultraviolet (UV) radiation induces intracellular production of hydrogen peroxide and causes activation of EGFR and ERK1/2 [10]. Both AG1478 and PP2 block the UV-induced activation of EGFR and ERK1/2 [11].

These results indicate the fundamental role of Src in the activation of EGFR and ERK1/2 following treatment with hydrogen peroxide and UV.

We considered the possibility that IR-induced intracellular hydrogen peroxide caused activation of EGFR and ERK1/2 through Src activation just as hydrogen peroxide and UV did. To investigate this, we studied the effects of IR on activities of ERK1/2, EGFR, SHP-2, Src, and PTP α as indicated by their tyrosine phosphorylation and effects of AG1478 and PP2 on them. In this report, we show IR-induced activation of ERK1/2, SHP-2, Src, and PTP α , and inhibition of IR-induced activation of ERK1/2 and SHP-2 by AG1478 and PP2, which suggests that IR-induced ERK1/2 activation is mediated through activation of Src/SHP-2 and EGFR.

Materials and methods

Reagents. Recombinant human epidermal growth factor (EGF) was purchased from Wako Pure Chemical Industries (Osaka, Japan). AG1478

* Corresponding author. Fax: +81 3 5841 3013.
E-mail address: hosoi@m.u-tokyo.ac.jp (Y. Hosoi).

and PP2 were obtained from Calbiochem (La Jolla, CA). Wortmannin was obtained from Sigma–Aldrich (St. Louis, MO). Anti-phospho-ERK1/2 (Thr202/Tyr204), anti-ERK1/2, anti-phospho-EGFR (Tyr845, Tyr992, Tyr1045, and Tyr1068), anti-phospho-SHP-2 (Tyr542), anti-SHP-2, anti-phospho-Src (Tyr416), and anti-phospho-PTP α (Tyr789) antibodies were purchased from Cell Signaling Technology (Beverly, MA). Anti-Src antibody was from Oncogene Research Products (San Diego, CA). Anti-EGFR antibody was from Transduction Laboratories (Lexington, KY). Anti- β -actin antibody was from Sigma (St. Louis, MO). A human breast cancer cell line MDA-MB-468 was obtained from American Type Culture Collection (Rockville, MD).

Cell culture, irradiation, and EGF treatment. Cells were cultured at 37 °C, 5% CO₂ in minimum essential medium (MEM) containing 10% fetal calf serum. Cells were plated at 5×10^5 cells in 60-mm dishes and incubated for 4 days without changing the culture medium. Cells were then treated with X-irradiation (200 kV, 20 mA, 0.5 mm Cu, and 1.0 mm Al filters, 1.36 Gy/min: HF-350C, SHIMADZU, Kyoto, Japan) or 10 ng/ml EGF. Cells were incubated at 37 °C for up to 6 h post the treatment and lysates were subjected to immunoblotting.

Immunoblotting. Cells were lysed in the electrophoresis sample buffer (62.5 mM Tris (pH 6.8), 2% SDS, 5% glycerol, 0.003% bromophenol blue, and 1% β -mercaptoethanol) and boiled for 5 min. The cell lysate was resolved by 7.5% polyacrylamide gel electrophoresis and was electrophoretically transferred to polyvinylidene difluoride membranes (Millipore, Bedford, MA). The membranes were then probed with antibodies and the antigen–antibody complexes were detected by the ECL Plus Western blotting detection reagents (Amersham Pharmacia Biotech, Piscataway, NJ) with horseradish peroxidase-conjugated antibodies.

Immunoprecipitation. Cells were washed with ice-cold Tris-buffered saline twice and incubated in lysis buffer (20 mM Hepes (pH 7.4), 150 mM NaCl, 1 mM EDTA, 1 mM EGTA, 1.0% Triton X-100, 0.5% deoxycholate (sodium salt), 1 mM sodium orthovanadate, 1 mM PMSF, and 1 μ g/ml leupeptin) for 20 min on ice. Cell lysates were then centrifuged at 13,500g for 10 min, the supernatants were incubated with protein G–Sepharose with primary antibody for 2 h. Following brief centrifugation, pellets were washed four times with lysis buffer and resuspended in loading buffer (125 mM Tris (pH 6.8), 4% SDS, 10% glycerol, 0.006% bromophenol blue, and 2% β -mercaptoethanol).

Results

Activation of ERK1/2 by ionizing radiation

First, we examined the effects of IR on ERK1/2 activity as indicated by its phosphorylation at Thr202/Tyr204. Irradiation with 0.5, 2, and 10 Gy caused an immediate ERK1/2 activation observed 2–5 min after irradiation followed by a late activation observed 6 h after irradiation (Fig. 1A). We further investigated the effects of IR on ERK1/2 activity with a wider dose range and found that irradiation with 0.1–20 Gy induced ERK1/2 activation (Fig. 1B).

Effects of AG1478, PP2, and wortmannin on IR-induced ERK1/2 activation

To investigate the signal transduction pathway involving IR-induced ERK1/2 activation, we studied effects of specific EGFR inhibitor AG1478 and specific Src inhibitor PP2 on IR-induced ERK1/2 activation. We first examined effects of AG1478 and PP2 on EGF-induced ERK1/2 activation to compare the IR-induced EGFR activation with the ligand-dependent one. AG1478 suppressed

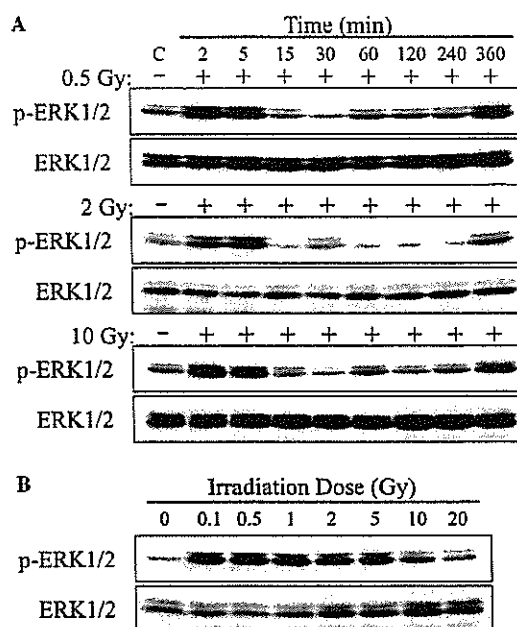


Fig. 1. ERK1/2 becomes phosphorylated at Thr202/Tyr204 in response to 0.1–20 Gy irradiation. (A) MDA-MB-468 cells were irradiated with 0.5, 2.0 or 10 Gy and incubated for 2–360 min at 37 °C. Whole cell lysates were then prepared and immunoblotted for phospho-ERK1/2 (Thr202/Tyr204) and ERK1/2. (B) MDA-MB-468 cells were irradiated with 0.1–20 Gy and incubated for 2 min at 37 °C. Whole cell lysates were then prepared and immunoblotted similarly.

EGF-induced ERK1/2 activation at 2–5 min after the addition of EGF into the culture medium but it failed to suppress the ERK1/2 activation later (Fig. 2A). PP2 did not suppress EGF-induced ERK1/2 activation (Fig. 2A). These results suggest that EGF-induced ERK1/2 activation is independent of Src. Next, we examined effects of AG1478 and PP2 on IR-induced ERK1/2 activation. AG1478 suppressed IR-induced ERK1/2 activation (Fig. 2B). PP2 suppressed the ERK1/2 activation observed 2–5 min after irradiation and partially suppressed the activation observed 360 min after irradiation (Fig. 2B). Although ERK1/2 activation has been linked to the activity of phosphatidylinositol-3 kinase (PI3K) in some system [12], we did not observe effects of PI3K-inhibition with wortmannin on IR-induced ERK1/2 activation (Fig. 2B). These results suggest that IR-induced ERK1/2 activation observed 2–5 min after irradiation is mediated by EGFR and Src.

IR-induced tyrosine phosphorylation of EGFR

Irradiation with 2 Gy induced immediate tyrosine phosphorylation observed 2–5 min after irradiation followed by a late tyrosine phosphorylation observed 6 h after irradiation (Fig. 3A). This time course of tyrosine phosphorylation corresponds to that of IR-induced ERK1/2 activation (Fig. 1A).

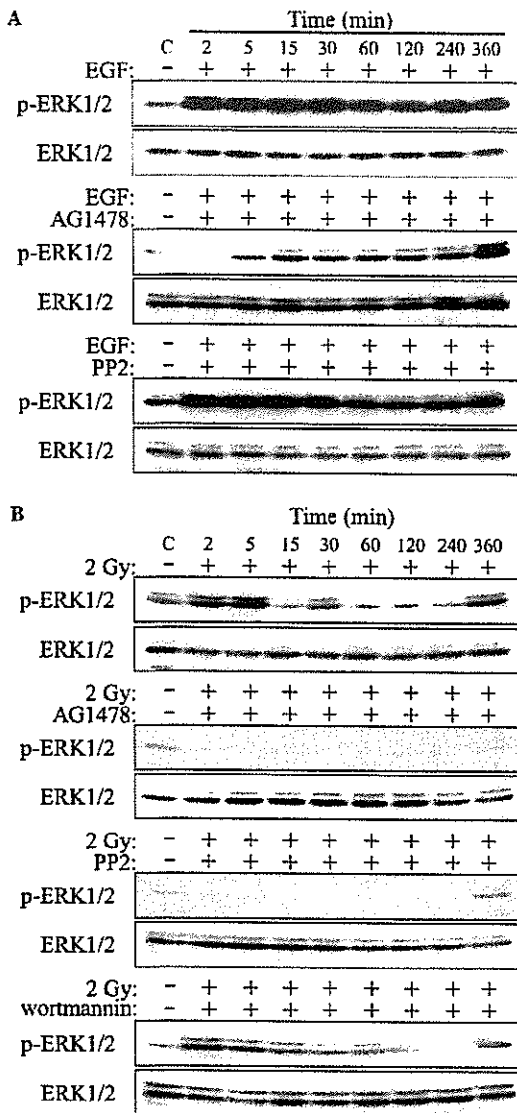


Fig. 2. Effects of AG1478, PP2 and wortmannin on ERK1/2 activation induced by EGF treatment or 2 Gy irradiation. MDA-MB-468 cells were treated with 0.5 μ M AG1478, 10 μ M PP2 or 200 nM wortmannin 30 min before the treatment with 10 ng/ml EGF (A) or 2 Gy irradiation (B). After the treatment with EGF or irradiation, cells were incubated for 2–360 min at 37 °C. Whole cell lysates were then prepared and immunoblotted for phospho-ERK1/2 (Thr202/Tyr204) and ERK1/2.

Effects of IR on EGFR phosphorylation at Tyr845, Tyr992, Tyr1045, and Tyr1068

For further investigation of EGFR phosphorylation after exposure to IR, we investigated IR-induced EGFR phosphorylation at Tyr845, Tyr992, Tyr1045, and Tyr1068 using antibodies specific to these phosphorylation sites of the activated EGFR. The phosphorylation at Tyr992, Tyr1045, and Tyr1068 has been reported to be mediated by EGFR tyrosine kinase and the phosphorylation at

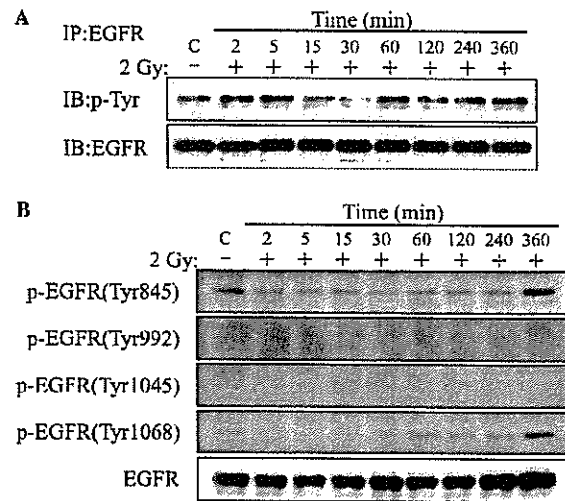


Fig. 3. Effects of IR on tyrosine phosphorylation of EGFR. MDA-MB-468 cells were irradiated with 2 Gy. After irradiation, cells were incubated for 2–360 min at 37 °C. Whole cell lysates were then prepared. (A) The whole cell lysates were subjected to immunoprecipitation with anti-EGFR antibody. The immunoprecipitates were immunoblotted for phosphotyrosine (p-Tyr) and EGFR. (B) The whole cell lysates were immunoblotted for phospho-EGFR (Tyr845, Tyr992, Tyr1045, and Tyr1068) and EGFR.

Tyr845 by Src [13,14]. Irradiation with 2 Gy caused a prompt decrease of EGFR phosphorylation at Tyr845 and Tyr1068 observed 2–15 min after irradiation followed by an increase of the phosphorylation observed 6 h after irradiation without obvious alteration of the phosphorylation at Tyr992 and Tyr1045 (Fig. 3B). In response to EGF stimulation, EGFR became phosphorylated at Tyr845, Tyr1068 (Fig. 4A), Tyr992, and Tyr1045 (data not shown). These data indicate that IR-mediated ERK1/2 activation involves an autophosphorylation-independent mechanism that is distinct from EGFR ligand activation.

Effects of AG1478 and PP2 on EGFR phosphorylation after EGF treatment or 2 Gy irradiation

Because EGFR phosphorylation at Tyr845 and Tyr1068 was affected by IR (Fig. 3B), we investigated effects of AG1478 and PP2 on EGF- and IR-induced phosphorylation at Tyr845 and Tyr1068 [13,14]. AG1478 partially suppressed EGF-induced phosphorylation and it suppressed IR-induced phosphorylation observed 6 h after irradiation (Figs. 4A and B). PP2 suppressed EGF- and IR-induced phosphorylation at Tyr845 but it failed to suppress the phosphorylation at Tyr1068 (Figs. 4A and B).

Irradiation with 2 Gy induces SHP-2 activation, which is inhibited by PP2

SHP-2 positively regulates the ability of several receptor tyrosine kinases (RTKs) to activate the Ras/Raf/ERK signaling cascade, and it plays a fundamental role in the regulation of Ras/Raf/ERK signaling from RTKs [15,16]. We

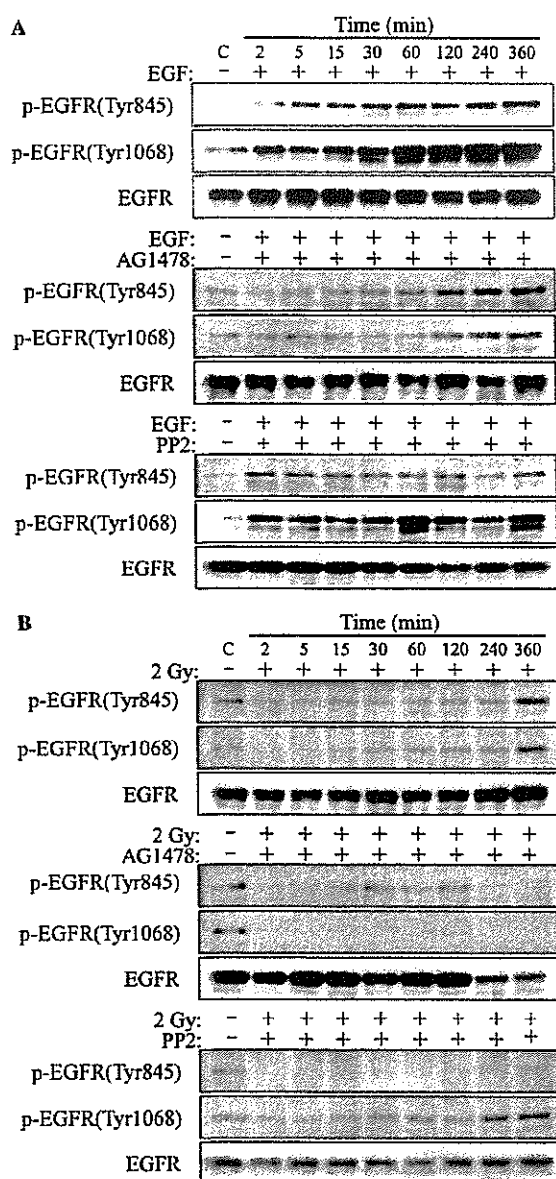


Fig. 4. Effects of AG1478 and PP2 on the phosphorylation status of EGFR after EGF treatment or 2 Gy irradiation. MDA-MB-468 cells were treated with 0.5 μ M AG1478 or 10 μ M PP2 30 min before the treatment with 10 ng/ml EGF (A) or 2 Gy irradiation (B). After the treatment with EGF or irradiation, cells were incubated for 2–360 min at 37 °C. Whole cell lysates were then prepared and immunoblotted for phospho-EGFR (Tyr845, Tyr1068) and EGFR.

examined if IR affected SHP-2 activity because Src and RTKs activate SHP-2 [16–18]. We first examined the effects of EGF on SHP-2 activity and found that SHP-2 became activated after EGF treatment as indicated by its phosphorylation at Tyr542 (Fig. 5A). AG1478 little affected EGF-induced phosphorylation of SHP-2, whereas PP2 suppressed the increased phosphorylation (Fig. 5A). These data indicate that EGF-induced SHP-2 activation is mainly

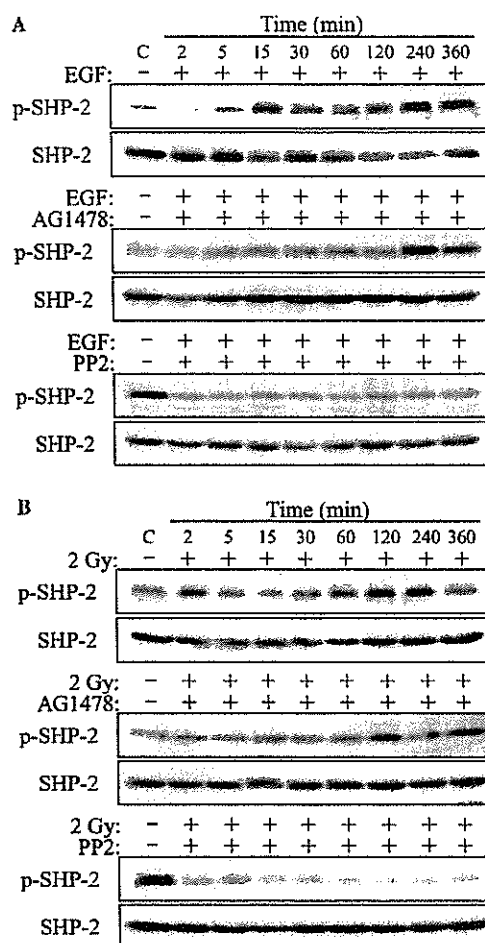


Fig. 5. SHP-2 becomes phosphorylated in response to 2 Gy irradiation and EGF, which is inhibited by PP2 and AG1478. MDA-MB-468 cells were treated with 0.5 μ M AG1478 or 10 μ M PP2 30 min before the treatment with 10 ng/ml EGF (A) or 2 Gy irradiation (B). After the treatment with EGF or irradiation, cells were incubated for 2–360 min at 37 °C. Whole cell lysates were then prepared and immunoblotted for phospho-SHP-2 (Tyr542) and SHP-2.

mediated by Src. Next, we examined effect of IR on SHP-2 activity. IR caused increased SHP-2 phosphorylation 2 min and 1–6 h after irradiation (Fig. 5B). This enhanced phosphorylation was little affected by AG1478 and suppressed by PP2, which suggests that IR-induced SHP-2 activation is also mediated by Src (Fig. 5B).

IR induces activation of Src and PTP α

Since PP2 inhibited IR-induced ERK1/2 and SHP-2 activation (Figs. 2B and 4B), we examined effects of IR on Src. Src became activated 1–6 h after 2 Gy irradiation as indicated by its phosphorylation at Tyr416 (Fig. 6). Next, we investigated the effect of IR on the activity of PTP α that activates Src by dephosphorylation at Tyr527 [19]. PTP α became activated 1–6 h after 2 Gy irradiation as indicated by its phosphorylation at Tyr789 (Fig. 6).

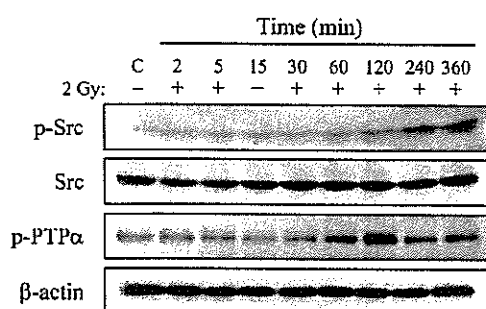


Fig. 6. Src and PTP α become phosphorylated in response to 2 Gy irradiation. MDA-MB-468 cells were irradiated with 2 Gy and incubated for 2–360 min at 37 °C. Whole cell lysates were then prepared and immunoblotted for phospho-Src (Tyr416), Src, phospho-PTP α (Tyr789), and β -actin.

Discussion

In the present study, IR activated PTP α , Src, SHP-2, EGFR, and ERK1/2. Src inhibitor PP2 suppressed activation of SHP-2 and ERK1/2, and EGFR inhibitor AG1478 suppressed activation of ERK1/2. These findings suggest that Src is an upstream signal for IR-induced ERK1/2 activation and are consistent with abundant evidence indicating that hydrogen peroxide evokes Src-dependent EGFR transactivation [20,21].

IR has been shown previously to activate EGFR, but the mechanism of the activation is not clear [1–3,22]. Our results indicate that IR activates EGFR via a mechanism that is distinct from EGFR autophosphorylation (Figs. 3 and 4). Ligand-independent transactivation of EGFR has been described with respect to a number of diverse stimuli including G-protein-coupled receptors, cytokines, and cellular stress [23]. The data presented here are in agreement with reports of H₂O₂-induced EGFR transactivation [20]. In that study, Src-activation by hydrogen peroxide induced EGFR-transactivation without phosphorylation of Tyr1173, an autophosphorylation site of the activated EGFR [20]. Our data indicate that IR induced EGFR tyrosine phosphorylation but does not involve EGFR phosphorylation at Tyr845, Tyr992, Tyr1045, and Tyr1068, which might be incompatible with EGFR activation (Fig. 3B). As Chen et al. [20] pointed out in their report, undescribed actions of AG1478 against Src kinase activity might be considered as potential explanations for these observations.

An important mechanism for regulation of Src tyrosine kinase activity is through control of its phosphorylation status [24]. The two major phosphorylation sites are an activating Tyr416 and an inhibiting Tyr527 [19,24]. PTP α has been demonstrated to dephosphorylate Src at Tyr527 and activate Src kinase activity [25]. In the present study, PTP α became activated 1–6 h after IR as indicated by its phosphorylation on Tyr789, which might be a cause of the Src activation observed 1–6 h after IR (Fig. 6). It is still unknown how PTP α is regulated during physiological

cellular signaling process. Protein kinase C is demonstrated to phosphorylate PTP α , which results in stimulation of its phosphatase activity [26,27]. Another mechanism by which regulates PTP α activity is dimerization that inhibits PTP α activity [27]. However, no physiological mechanism has been demonstrated through which the formation of the dimers can occur.

SHP-2 is a well-known positive effector of EGFR signaling [16,28,29]. In the present study, SHP-2 became activated 2 min and 1–6 h after irradiation and this activation was inhibited by PP2 (Fig. 5). The time course of IR-induced SHP-2 activation partially corresponds with that of IR-induced ERK1/2 activation. These data suggest that IR-induced ERK1/2 activation involves Src-dependent SHP-2 activation.

ERK1/2 activation observed 2–5 min after irradiation is suggested to be mediated through Src because PP2 inhibited the activation (Figs. 3B and 5B). However, Src became activated only 1–6 h after irradiation without apparent activation at 2–5 min post irradiation as indicated by its phosphorylation at Tyr416 (Fig. 6). One possible mechanism of this discrepancy is the Src activation by SHP-2 without increasing Src phosphorylation at Tyr416. Walter et al. [30] reported that SHP-2 activates Src by a non-enzymatic mechanism without significant changes in phosphorylation status of Src and that a phosphatase-inactive mutant of SHP-2 can also activate Src. Src activates SHP-2 by phosphorylating SHP-2 tyrosine residue with physically association with SHP-2 [17,18]. In this study, PP2 inhibited enhanced phosphorylation of SHP-2 observed 2 min after irradiation, which might indicate Src activation at 2 min after irradiation without increased phosphorylation at Tyr416. Another potential explanation for inhibition of IR-induced ERK1/2 activation by PP2 without increased Src phosphorylation at Tyr416 is undescribed action of PP2 against unknown kinase activities that mediate IR-induced ERK1/2 activation.

In summary, our data suggest that IR activates Src/SHP-2. This Src/SHP-2 activation mediates EGFR transactivation that causes Ras/Raf/ERK signaling cascade activation. However, it remains to be elucidated how Src and SHP-2 become activated in response to IR.

References

- [1] R.K. Schmidt-Ullrich, K. Valerie, P.B. Fogleman, J. Walters, Radiation-induced autophosphorylation of epidermal growth factor receptor in human malignant mammary and squamous epithelial cells, *Radiat. Res.* 145 (1996) 81–85.
- [2] R.K. Schmidt-Ullrich, R.B. Mikkelsen, P. Dent, D.G. Todd, K. Valerie, B.D. Kavanagh, J.N. Contessa, W.K. Rorrer, P.B. Chen, Radiation-induced proliferation of the human A431 squamous carcinoma cells is dependent on EGFR tyrosine phosphorylation, *Oncogene* 15 (1997) 1191–1197.
- [3] T. Goldkorn, N. Balaban, M. Shannon, K. Matsukuma, EGFR receptor phosphorylation is affected by ionizing radiation, *Biochim. Biophys. Acta* 1358 (1997) 289–299.
- [4] J.N. Contessa, J. Hampton, G. Lammering, R.B. Mikkelsen, P. Dent, K. Valerie, R.K. Schmidt-Ullrich, Ionizing radiation activates ErbB-

- receptor dependent Akt and p70 S6 kinase signaling in carcinoma cells, *Oncogene* 21 (2002) 4032–4041.
- [5] G.P. Amorino, V.M. Hamilton, K. Valerie, P. Dent, G. Lammering, R.K. Schmidt-Ullrich, Epidermal growth factor receptor dependence of radiation-induced transcription factor activation in human breast carcinoma cells, *Mol. Biol. Cell* 13 (2002) 2233–2244.
- [6] K. Sato, T. Nagao, T. Iwasaki, Y. Nishihira, Y. Fukami, Src-dependent phosphorylation of the EGF receptor Tyr-845 mediates Stat-p21waf1 pathway in A431 cells, *Genes Cells* 8 (2003) 995–1003.
- [7] S. Zhuang, R.G. Schnellmann, H₂O₂-induced transactivation of EGF receptor requires Src and mediates ERK1/2, but not Akt, activation in renal cells, *Am. J. Physiol. Renal Physiol.* 286 (2004) F858–F865.
- [8] S. Purdom, Q.M. Chen, Epidermal growth factor receptor-dependent and -independent pathways in hydrogen peroxide-induced mitogen-activated protein kinase activation in cardiomyocytes and heart fibroblasts, *J. Pharmacol. Exp. Ther.* 312 (2005) 1179–1186.
- [9] S. Zhuang, Y. Yan, J. Han, R.G. Schnellmann, p38 Kinase-mediated transactivation of the epidermal growth factor receptor is required for dedifferentiation of renal epithelial cells following oxidant injury, *J. Biol. Chem.* 280 (2005) 21036–21042.
- [10] D. Peus, A. Meves, R.A. Vasa, A. Beyerle, T. O'Brien, M.R. Pittelkow, H₂O₂ is required for UVB-induced EGF receptor and downstream signaling pathway activation, *Free Radic. Biol. Med.* 27 (1999) 1197–1202.
- [11] D. Kitagawa, S. Tanemura, S. Ohata, N. Shimizu, J. Seo, G. Nishitai, T. Watanabe, K. Nakagawa, H. Kishimoto, T. Wada, T. Tezuka, T. Yamamoto, H. Nishina, T. Katada, Activation of extracellular signal-regulated kinase by ultraviolet is mediated through Src-dependent epidermal growth factor receptor phosphorylation. Its implication in an anti-apoptotic function, *J. Biol. Chem.* 277 (2002) 366–371.
- [12] L.K. Robertson, L.R. Mireau, H.L. Ostergaard, A role for phosphatidylinositol 3-Kinase in TCR-stimulated ERK activation leading to Paxillin phosphorylation and CTL degranulation, *J. Immunol.* 175 (2005) 8138–8145.
- [13] M. Rojas, S. Yao, Y.Z. Lin, Controlling epidermal growth factor (EGF)-stimulated Ras activation in intact cells by a cell-permeable peptide mimicking phosphorylated EGF receptor, *J. Biol. Chem.* 271 (1996) 27456–27461.
- [14] J.S. Biscardi, M.C. Maa, D.A. Tice, M.E. Cox, T.H. Leu, S.J. Parsons, c-Src-mediated phosphorylation of the epidermal growth factor receptor on Tyr845 and Tyr1101 is associated with modulation of receptor function, *J. Biol. Chem.* 274 (1999) 8335–8343.
- [15] C.K. Qu, W.M. Yu, B. Azzarelli, G.S. Feng, Genetic evidence that Shp-2 tyrosine phosphatase is a signal enhancer of the epidermal growth factor receptor in mammals, *Proc. Natl. Acad. Sci. USA* 96 (1999) 8528–8533.
- [16] Y.M. Agazie, M.J. Hayman, Molecular mechanism for a role of SHP2 in epidermal growth factor receptor signaling, *Mol. Cell. Biol.* 23 (2003) 7875–7886.
- [17] G.S. Feng, C.C. Hui, T. Pawson, SH2-containing phosphotyrosine phosphatase as a target of protein-tyrosine kinases, *Science* 259 (1993) 1607–1611.
- [18] Z.Y. Peng, C.A. Cartwright, Regulation of the Src tyrosine kinase and Syp tyrosine phosphatase by their cellular association, *Oncogene* 11 (1995) 1955–1962.
- [19] J.D. Bjorge, A. Jakymiw, D.J. Fujita, Selected glimpses into the activation and function of Src kinase, *Oncogene* 19 (2000) 5620–5635.
- [20] K. Chen, J.A. Vita, B.C. Berk, J.F. Keaney Jr, c-Jun N-terminal kinase activation by hydrogen peroxide in endothelial cells involves SRC-dependent epidermal growth factor receptor transactivation, *J. Biol. Chem.* 276 (2001) 16045–16050.
- [21] K.K. Griendling, D. Sorescu, B. Lassegue, M. Ushio-Fukai, Modulation of protein kinase activity and gene expression by reactive oxygen species and their role in vascular physiology and pathophysiology, *Arterioscler. Thromb. Vasc. Biol.* 20 (2000) 2175–2183.
- [22] R.K. Schmidt-Ullrich, J.N. Contessa, G. Lammering, G. Amorino, P.S. Lin, ERBB receptor tyrosine kinases and cellular radiation responses, *Oncogene* 22 (2003) 5855–5865.
- [23] E. Zwick, P.O. Hackel, N. Prenzel, A. Ullrich, The EGF receptor as central transducer of heterologous signalling systems, *Trends Pharmacol. Sci.* 20 (1999) 408–412.
- [24] R. Roskoski Jr, Src kinase regulation by phosphorylation and dephosphorylation, *Biochem. Biophys. Res. Commun.* 331 (2005) 1–14.
- [25] J. den Hertog, C.E. Pals, M.P. Peppelenbosch, L.G. Tertoolen, S.W. de Laat, W. Kruijer, Receptor protein tyrosine phosphatase alpha activates pp60c-src and is involved in neuronal differentiation, *EMBO J.* 12 (1993) 3789–3798.
- [26] J. den Hertog, J. Sap, C.E. Pals, J. Schlessinger, W. Kruijer, Stimulation of receptor protein-tyrosine phosphatase alpha activity and phosphorylation by phorbol ester, *Cell Growth Differ.* 6 (1995) 303–307.
- [27] S. Tracy, P. van der Geer, T. Hunter, The receptor-like protein-tyrosine phosphatase, RPTP alpha, is phosphorylated by protein kinase C on two serines close to the inner face of the plasma membrane, *J. Biol. Chem.* 270 (1995) 10587–10594.
- [28] N.K. Tonks, B.G. Neel, Combinatorial control of the specificity of protein tyrosine phosphatases, *Curr. Opin. Cell Biol.* 13 (2001) 182–195.
- [29] L.M. Sturla, G. Amorino, M.S. Alexander, R.B. Mikkelsen, K. Valerie, R.K. Schmidt-Ullrich, Requirement of Tyr-992 and Tyr-1173 in phosphorylation of the epidermal growth factor receptor by ionizing radiation and modulation by SHP2, *J. Biol. Chem.* 280 (2005) 14597–14604.
- [30] A.O. Walter, Z.Y. Peng, C.A. Cartwright, The Shp-2 tyrosine phosphatase activates the Src tyrosine kinase by a non-enzymatic mechanism, *Oncogene* 18 (1999) 1911–1920.